BIOCHEMISTRY
including biophysical chemistry & molecular biology
Article

Biochemistry **2010,** *49,* 7949–7955 7949
DOI: 10.1021/bi1010255

Structural Basis for the Specificity of the GAE Domain of yGGA2 for Its Accessory Proteins Ent3 and Ent5[†,‡]

Pengfei Fang, Xu Li, Jing Wang, Liwen Niu,* and Maikun Teng*

Hefei National Laboratory for Physical Sciences at Microscale and School of Life Sciences, University of Science and Technology of China, Anhui 230026, China, and Key Laboratory of Structural Biology, Chinese Academy of Sciences, 96 Jinzhai Road, Hefei, Anhui 230026, China

Received June 26, 2010; Revised Manuscript Received August 4, 2010

ABSTRACT: Different assemblies of accessory proteins with clathrin are critical for transporting precisely various cargos between intracellular compartments. GGA proteins are adaptors for clathrin-mediated intracellular trafficking, connecting other accessory and cargo proteins to clathrin-coated vesicles. Both binding to the GAE domain of GGA protein yGGA2 in *Saccharomyces cerevisia*, Ent3 and Ent5 are involved in different trafficking pathways. Ent5 is ubiquitous and localized in a manner independent of yGGA2, and Ent3 functions preferentially through yGGA2. Not known are the sources of these differences. Here we show not all acidic-phenylalanine motifs in Ent3/5 are active for yGGA2_GAE domain binding. Two of the three acidic-phenylalanine motifs from Ent3 can bind to the yGGA2_GAE domain, while only one of the two motifs from Ent5 can bind. We also determined the crystal structure of the yGGA2_GAE domain at 1.8 Å resolution. Structural docking and mutagenesis analysis shows inactive motifs in Ent3 and Ent5 repel yGGA2_GAE binding through disfavored residues at positions 1 and 3. These results suggest accessory proteins may fine-tune the GGA adaptor dependence by adjusting their non-acidic-phenylalanine residues, thus contributing to the distinct role of Ent3 and Ent5 in trafficking.

Clathrin-coated vesicles are responsible for lipid and protein transport between intracellular, membrane-bound compartments and also play a key role in endocytosis (*1*). Its assembly involves clathrin-binding adaptors. Three classes of adaptors participate in clathrin-coated vesicle-mediated traffic in mammalian and yeast cells: AP proteins, GGA proteins,[1] and epsin-like proteins. They anchor the nascent coat to cargo proteins or to the membrane through its association with lipids and, thus, are central to the process of vesicle formation (*2*).

The GGA proteins are monomeric adaptors that contain a C-terminal domain (GAE domain) homologous to the γ-ear domain of AP-1. The GAE/γ-ear domain from both GGA and AP-1 can bind and recruit a number of accessory proteins and contribute to coated vesicle biogenesis (*3*, *4*). There are two GGA proteins (yGGA1 and yGGA2) in yeast and three (GGA1−3) in humans with possibly redundant functions. In humans, the accessory proteins recruited by GAE domains include γ-synergin, Rabaptin-5, p56, epsinR, epsin1, and epsin2 (*5*). In yeast, yGGA2 is expressed at 5−10-fold higher levels than yGGA1 (*6*). Ent3 and Ent5 are the only known partners of the yGGA2_GAE domain (*7*). AP-1 in yeast also helps to determine the localization of Ent5 in the cell (*11*). A similar GGA-binding protein, epsinR, exists in mammalian cells. Ent3 and Ent5 belong to the ENTH/ANTH family that could directly interact with phosphoinositides and lead to the membrane localization and promote membrane curvature (*8*). In addition, Ent3 also functions as an adaptor for SNARE proteins like Pep12 and Vti1 in a yGGA2-dependent manner (*9*). Meanwhile, Ent5 binds to a multipass membrane protein Chs3 (*10*). Thus, the interactions of Ent3 and Ent5 and adaptors play an important role in their clathrin-related functions.

Although Ent3 and Ent5 share similar sequences (Figure 1A), they have distinct functions in vesicle-mediated traffic. In yGGA-deficient cells, synthetic genetic growth and α-factor maturation defects were observed with ent5Δ but not with ent3Δ. In AP-1-deficient cells, ent3Δ caused more α-factor maturation defects than ent5Δ (*11*). Ent3 is preferentially localized with yGGA2, whereas Ent5 is more critical for AP-1-mediated transport and is distributed equally between AP-1 and yGGA2 (*10*, *11*). Ent3 is mislocalized in yGGA-deficient but not in AP-1-deficient cells. In contrast, Ent5 retained localization in cells lacking either AP-1, GGA, or both (*11*). Therefore, it was suggested that direct interactions between GAE domains and Ent3 and Ent5 play an important role in the distinct function between Ent3 and Ent5 (*11*).

An acidic-phenylalanine motif "$[D/E]_nFxx\Phi$" (Φ represents any hydrophobic amino acid; x represents any residue) was characterized as the consensus binding site for GAE domains and the γ-ear domain of AP-1 (*5*, *7*, *12*−*15*). It contains an invariant phenylalanine (position 0) following a string of acidic residues $(D/E)_{3-9}$. Several bulky hydrophobic residues (for example, Phe, Met, and Leu)

[†]This project was supported by research grants from the Chinese National Natural Science Foundation (Grants 30025012 and 10979039), the Chinese Ministry of Science and Technology (Grants 2006CB806500, 2006CB910200, and 2006AA02A318), the Chinese Academy of Sciences (Grant KSCX2-YW-R-60), the Chinese Ministry of Education (Grant 20070358025), and the Anhui Provincial Natural Science Foundation (Grant 090413081).

[‡]The coordinates and structure factors have been deposited in the Protein Data Bank as entry 3MNM.

*To whom correspondence should be addressed. E-mail: lwniu@ustc.edu.cn or mkteng@ustc.edu.cn. Telephone and fax: 86-551-3606314.

[1]Abbreviations: ANTH domain, AP180 N-terminal homology domain; AP-1, assembly protein complex 1; ENTH domain, epsin N-terminal homology domain; GAE domain, γ-adaptin ear domain; GGA proteins, Golgi-localizing, γ-adaptin ear domain-containing, ADP ribosylation factor (ARF)-binding proteins; rmsd, root-mean-square deviation.

Published on Web 08/12/2010

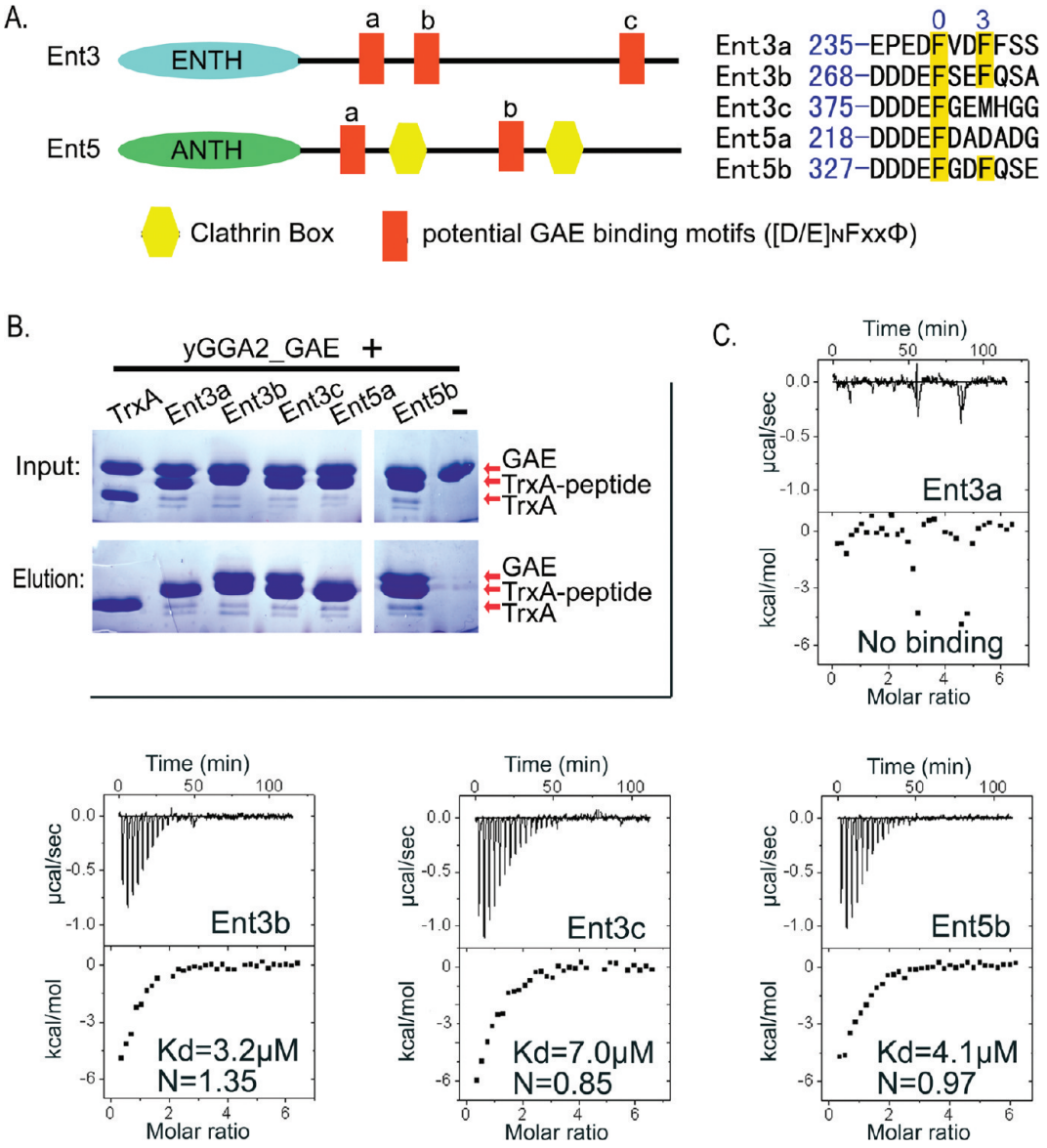

FIGURE 1: Interaction of acidic-phenylalanine motifs in Ent3 and Ent5 with the yGGA2_GAE domain. (A) Domain scheme of Ent3 and Ent5. The acidic-phenylalanine motifs in Ent3 and Ent5 are aligned on the right. The first phenylalanine in each motif is designated Phe0. (B) Pull-down assays of the TrxA-fused acidic-phenylalanine motifs and yGGA2_GAE domain interaction. (C) ITC experiments with the TrxA-fused acidic-phenylalanine motifs and yGGA2_GAE domain interaction.

have been found at position 3, with high level of diversity at other positions (*7*). On the basis of this criterion, several acidic-phenylalanine motifs were proposed on Ent3 and Ent5 (*5*, *7*). However, the mechanism of how Ent3 and Ent5 bind differently to yGGA2 remains unclear. Here we studied the interaction between these motifs in Ent3 and Ent5 and the yGGA2_GAE domain in detail. We found two of the three acidic-phenylalanine motifs in Ent3 are able to bind the yGGA2_GAE domain independently, while only one of two motifs in Ent5 can bind. We further determined the crystal structure of the yGGA2_GAE domain at 1.8 Å resolution. On the basis of the structural analysis, docking simulation, and binding assays, we showed switching the residues at positions 1 and 3 in these acidic-phenylalanine motifs could turn on or off their GGA2_GAE binding. While the acidic-phenylalanine residues are essential for accessory proteins to interact with GAE/γ-ear domains of adaptors, our results indicated sequences at positions 1 and 3 are used by nature to fine-tune their specificity for GAE domains and could contribute to the distinct roles of Ent3 and Ent5 in trafficking.

METHODS

Cloning, Expression, and Purification. The gene fragment encoding yGGA2_GAE (UniProtKB entry P38817, residues 465−585) was amplified from *Saccharomyces cerevisiae* genome DNA and cloned into a modified pET22b+ plasmid. Native and Se-Met-derived yGGA2_GAE are prepared similarly in LB or M9 medium. yGGA2_GAE was overexpressed in B834(DE3) (Merck, Shanghai, China) with an MGHHHHHHMEN-LYFQSL tag fused to its N-terminus, and with IPTG induction at 16 °C. Affinity chromatography with a Chelating Sepharose Fast Flow column (Amersham Biosciences, Uppsala, Sweden) was used as the first step of the purification. The protein was eluted with elution buffer [20 mM Tris-HCl (pH 7.5), 400 mM NaCl, and 500 mM imidazole]. It was then changed to 20 mM Tris-HCl (pH 7.5), 5 mM EDTA, and 10 mM 2-mercaptoethanol to cleave the His tag using TEV protease at 16 °C. The sample was then changed to 20 mM Tris-HCl (pH 7.5), 400 mM NaCl, and 40 mM imidazole. It was then passed through a chelating affinity chromatography column to remove the TEV protease.

Table 1: Data Collection, Phasing, and Refinement Statistics

	native	Se-MAD		
		peak	inflection	remote
Data Collection[a]				
space group	$P4_32_12$		$P4_22_12$	
cell dimensions (Å)	$a = b = 89.72$, $c = 117.03$		$a = b = 152.23$, $c = 70.47$	
wavelength (Å)	1.0	0.9789	0.9792	0.9000
resolution (Å)	50−1.73 (1.76−1.73)		20−3.00 (3.11−3.00)	
R_{sym} or R_{merge}[b]	6.6 (49.7)	11.0 (38.8)	11.5 (46.2)	17.3 (79.0)
$I/\sigma I$	43.2 (4.4)	31.9 (5.6)	25.2 (4.7)	15.1 (2.1)
completeness (%)	100 (99.9)	99.3 (97.4)	99.5 (98.9)	99.5 (98.1)
redundancy	14.2 (10.4)	26.5 (21.0)	26.9 (23.2)	24.5 (13.7)
Refinement				
resolution (Å)	50−1.73 (1.78−1.73)			
no. of reflections	47880 (2567)			
R_{work},[c] R_{free}[d]	19.7 (28.0), 22.9 (34.6)			
no. of atoms				
protein	2598			
ligand/ion	45			
water	322			
B-factor				
protein	23.54			
ligand/ion	37.49			
water	32.76			
rmsd				
bond lengths (Å)	0.007			
bond angles (deg)	1.143			
Ramachandran plot (%)				
most favored regions	90.4			
additional allowed regions	9.6			

[a]Values in parentheses are for the highest-resolution shell. [b]$R_{merge} = \sum_h\sum_l|I(h)_l - \langle I(h)\rangle|/\sum_h\sum_l I(h)_l$, where $I(h)_l$ is the lth observation of reflection h and $\langle I(h)\rangle$ is the weighted average intensity for all observations l of reflection h. [c]$R_{work} = \sum_h||F_{obs}(h)| - |F_{cal}(h)||/\sum_h|F_{obs}(h)|$, where $F_{obs}(h)$ and $F_{cal}(h)$ are the observed and calculated structure factors for reflection h, respectively. [d]R_{free} was calculated as R_{work} using the 5% of the reflections that were selected randomly and omitted from refinement.

The sample was then changed to 50 mM Na-Hepes (pH 7.5) and 200 mM NaCl for lysine methylation (*16*). After lysine methylation, a Superdex 75 column (16 mm × 120 mm, Amersham Biosciences) was used to further purify methylated yGGA2_GAE. The protein was then concentrated to 10 mg/mL in distilled water for crystallization.

Different peptides derived from the acidic-phenylalanine motifs of Ent3 and Ent5 were constructed by fusion with an eight-His-tagged *Escherichia coli* thioredoxin protein TrxA at the N-terminus (Table S1 of the Supporting Information). Proteins used in isothermal titration microcalorimetry (ITC) and His-tag pull-down assays were overexpressed in BL21(DE3) (Merck) and purified by affinity chromatography. Buffer for all samples was changed to 20 mM Tris-HCl (pH 7.5) with 200 mM NaCl using a size exclusion chromatography column with a Superdex 75 column.

Isothermal Titration Calorimetry (ITC) Experiments. ITC experiments were performed on a MicroCal VP ITC unit at 25 °C (MicroCal, Piscataway, NJ). The buffer for all proteins consisted of 20 mM Tris-HCl (pH 7.5) and 200 mM NaCl. Aliquots of the yGGA2_GAE solution (8 μL) were injected from a 287 μL rotating syringe (307 rpm) into the isothermal sample chamber containing 1.43 mL of a TrxA-fused peptide solution. Corresponding control experiments to determine the heat of dilution of yGGA2_GAE to buffer were performed similarly. The area under each peak was determined by integration using Origin 7.0 to give a measure of the heat associated with the injection. The resulting data were analyzed to estimate the binding affinity (K_d).

His-Tag Pull-Down Assay. Each TrxA peptide (eight-His-tagged) was incubated with yGGA2-GAE (without the His tag) in 20 mM Tris-HCl (pH 7.5) and 200 mM NaCl. The mixture was then passed through a chelating affinity column. The column was then washed with the buffer containing 20 mM Tris-HCl (pH 7.5), 200 mM NaCl, and 20 mM imidazole. The protein was eluted with the buffer containing 20 mM Tris-HCl (pH 7.5), 200 mM NaCl, and 100 mM EDTA. The result was checked by SDS−PAGE and stained with Coomassie blue.

Crystallization and Data Collection. Native and Se-Met-derived crystals were prepared similarly. Crystallization of the yGGA2_GAE protein (native or Se-Met-derived) was performed at 15 °C using the hanging drop vapor diffusion method, and initial trials were conducted using Crystal Screen I and Crystal Screen II reagent kits (Hampton Research, Aliso Viejo, CA). Each hanging drop was a mixture of 2 μL of protein and an equal volume of reservoir solution. It was then equilibrated against 200 μL of reservoir solution. After 5−7 days, crystals in 0.5 M ammonium sulfate, 0.1 M trisodium citrate (pH 5.6), and 1.0 M lithium sulfate grew to a size suitable for X-ray diffraction.

Native crystals were then soaked in a cryoprotection solution [0.375 M ammonium sulfate, 0.075 M trisodium citrate (pH 5.6), 0.75 M lithium sulfate, and 25% glycerol] prior to data collection.

X-ray diffraction data of the native crystal were collected on beamline 17U1 of the Shanghai Synchrotron Radiation Facility (SSRF). X-ray diffraction data of the Se-Met-derived crystal were collected on beamline 3W1A of the Beijing Synchrotron Radiation Facility (BSRF). This crystal was passed through paraffin oil for cryoprotection. All diffraction data were processed and scaled with HKL2000 (*17*).

Phase Determination and Structure Refinement. The original model was built using the Se-Met-derived diffraction data by the multiple-anomalous diffraction (MAD) method using SOLVE/RESLOVE (*18*, *19*). It was then used as a search model for native data by molecular replacement in Molrep (*20*). Iterative model building and refinement were conducted with Coot (*21*), CNS (*22*), and Refmac5 (*23*) with TLS and restrained refinement (*24*). The quality of the final model was checked with Procheck (*25*). The current model has good geometry and no residues in disallowed regions in the Ramachandran plot. Data collection and refinement statistics are listed in Table 1. Figures were prepared using PyMOL (http://www.pymol.org/).

Structural Docking of the Acidic-Phenylalanine Motifs of Ent3 and Ent5 on GGA2_GAE. The initial binding site of the acidic-phenylalanine motifs on the GAE domain was determined according to the complex structure of the human GGA1_GAE domain with the WNSF motif [Protein Data Bank (PDB) entry 2dwx]. The structure of the monomeric yGGA2_GAE domain was superimposed onto that of the human GGA1_GAE domain. The peptides from Ent3 (EFSEFQSA) and Ent5 (EFGDFQSE) were placed at the WNSF motif-binding site. These yGGA2_GAE−peptide complexes were optimized by molecular dynamics simulation using GROMACS (*26*). The GROMOS96 force field was used to perform the simulations, with 1000 steps of steepest-descent energy minimization to achieve the convergence of binding.

RESULTS

Functional GAE-Binding Motifs: Two in Ent3 and One in Ent5. On the basis of the consensus acidic-phenylalanine sequence, different numbers of potential yGGA2_GAE-binding motifs on Ent3 and Ent5 have been proposed (*5*, *7*). In total, there are three acidic-phenylalanine motifs in Ent3 with potential for binding to yGGA2, and two in Ent5 (Figure 1A). They are "235EPEDFVDFFSS" (Ent3a), "268DDDEFSEFQSA" (Ent3b), "375DDDEFGEMHGG" (Ent3c), "218DDDEFDADADG" (Ent5a), and "327DDDEFGDFQSE" (Ent5b). These acidic-phenylalanine motifs have consensus acidic residues followed by an invariant phenylalanine [this first phenylalanine in each motif is designated as Phe0 (Figure 1A)]. Little similarity was found at other positions, with the exception of a predominant phenylalanine at position 3. Mutation of phenylalanines to alanines in the last two motifs (Ent3b and Ent3c) reduced the level of Ent3−yGGA2 binding to background levels in two-hybrid analysis (*7*). However, no direct study of the interaction of each potential binding motif with yGGA2_GAE has been conducted, and the real binding site(s) has not been identified.

To gain a clear understanding of the functional difference between Ent3 and Ent5 and their connection with yGGA2-dependent clathrin assembly, we constructed five fused proteins with each acidic-phenylalanine motif at the C-terminus of an *E. coli* TrxA protein (Table S1 of the Supporting Information). Pull-down experiments using these TrxA-fused peptides showed a distinct behavior for each acidic-phenylalanine motif. Only

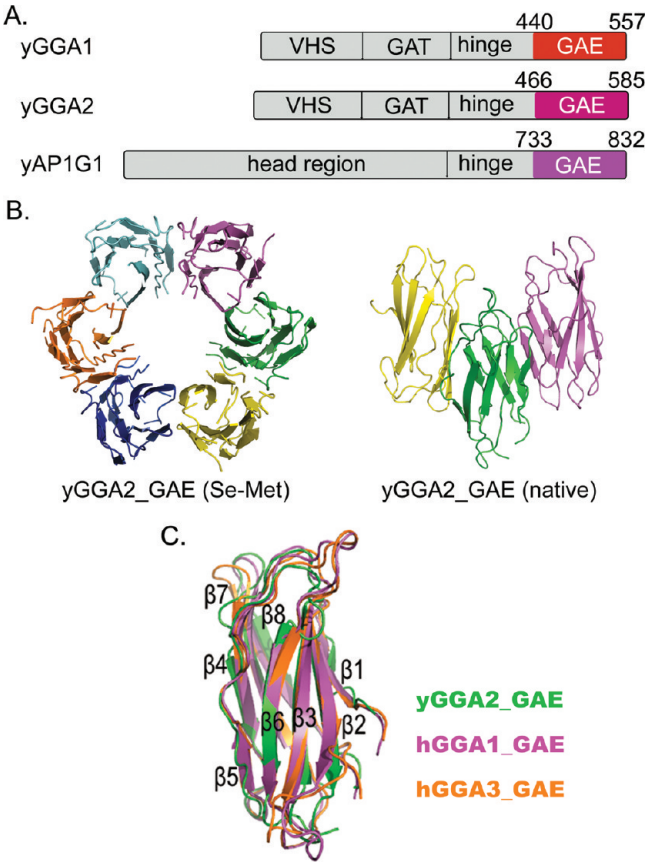

FIGURE 2: Crystal structure of the yGGA2_GAE domain. (A) Domain scheme of GAE-containing proteins in yeast. (B) Molecular packing in an asymmetric unit in Se-Met-derived crystals and native crystals. (C) Structure superimposition of yGGA2_GAE with human GGA1_GAE (PDB entry 2dwx) and human GGA3_GAE (PDB entry 1p4u).

Ent3b, Ent3c, and Ent5b can bind to the yGGA2_GAE domain (Figure 1B), while Ent3a and Ent5a had no any detectable binding. We then further verified this result by quantitative ITC. The ITC experiment showed Ent3b, Ent3c, and Ent5b bind to the yGGA2_GAE domain with similar affinities of 3−7 μM, which is close to or higher than the affinities of other known GAE domain−acidic-phenylalanine motif complexes (*12*, *27*). Again no binding of Ent3a and Ent5a to yGGA2_GAE was detected, even at a yGGA2_GAE concentration of 0.8 mM (Figure 1C; also see Figure 3C). A decrease of at least 100-fold was estimated for Ent3a and Ent5a compared with Ent3b/c and Ent5b. Thus, not all acidic-phenylalanine motifs in Ent3 and Ent5 are functional. In spite of having the consensus $(D/E)_nF$ sequence, these motifs in Ent3 and Ent5 possess a considerable difference in binding to yGGA2_GAE.

Crystal Structure of the yGGA2_GAE Domain. To further identify the extra determinants that govern the specific binding of these acidic-phenylalanine motifs to the GAE domain, we set out to determine the crystal structure of the yGGA2_GAE domain (Figure 2A). With the treatment of lysine methylation, we crystallized the yGGA2_GAE domain in two different forms at 1.8 Å resolution. In an asymmetric unit of the Se-Met-derived crystals (space group $P4_22_12$), there are six molecules forming a hexagonal ring structure. In native crystals ($P4_32_12$), the asymmetric unit contains only three molecules similar to half of the hexagonal ring (Figure 2B). Previous research showed the GGAs are monomeric proteins (*3*, *28*), the one exception being that the human GGA1_GAE forms a homodimer in solution (*27*). Thus, we checked the solution state of the yGGA2_GAE domain via

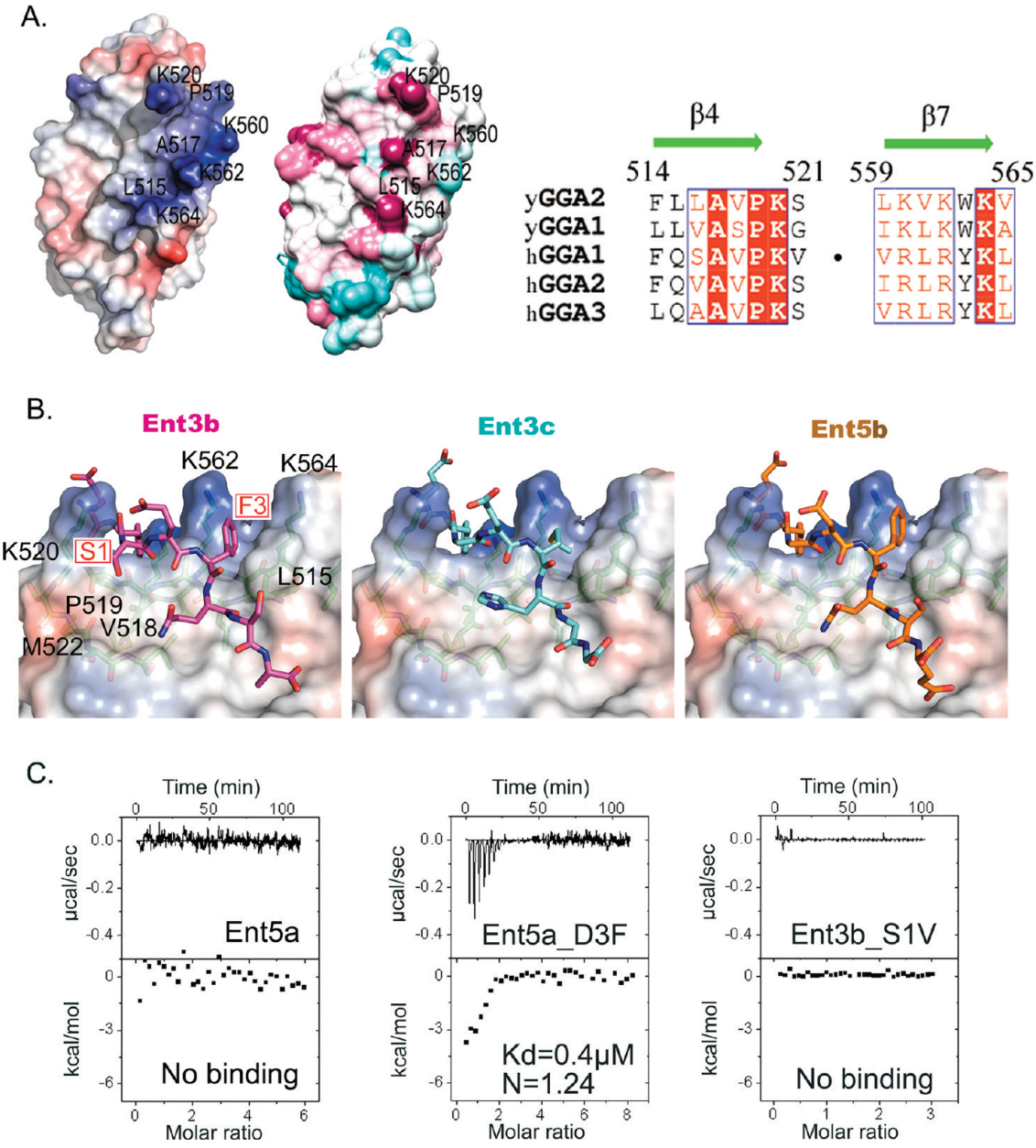

FIGURE 3: Fine specificity of GGA2_GAE binding that depends on the sequence of positions 1 and 3 in the acidic-phenylalanine motifs. (A) Electrostatic distribution on molecular surface of yGGA2_GAE (left). Sequence conservation in the GGA family is also marked on the molecular surface (middle): red for conserved residues, light cyan for less conserved, and white for even less conserved. Residues forming the peptide-binding site are labeled. β4 and β7 are involved in binding, and their sequences from the GGA family are aligned (right). (B) Docking of Ent3 and Ent5 motifs to the yGGA2_GAE structure. S1 and F3 indicate the position 1 and 3 residues of Ent3b, respectively. All models are shown in the same orientation. (C) ITC experiments with mutants Ent3a_D3F and Ent3b_S1V binding to yGGA2_GAE.

size exclusion chromatography. The calculated molecular mass of the yGGA2_GAE domain is 16 kDa, close to the molecular mass of the monomeric form [13 kDa (Figure S1 of the Supporting Information)].

The structure of yGGA2_GAE shows a β-sandwich fold composed of eight β-strands [β1-β2-β3-β5-β6 and β4-β7-β8 (Figure 2C)]. It resembles the eight-strand β-sandwich scaffold of previously determined human GAE domains (*12*, *27*, *29*), with rmsd values of 1.8 Å with respect to human GGA1_GAE and 2.0 Å with respect to GGA3_GAE (Figure 2C), despite their low levels of sequence identity (22 and 20%, respectively). This similarity between GAE structures allowed us to model peptide binding on the yeast GGA2_GAE domain.

Modeling of Acidic-Phenylalanine Motifs of Ent3 and Ent5 on yGGA2_GAE. Both the human GGA1_GAE domain and the human GGA3_GAE domain bind their partner peptides in the same region on strands β4 and β7 (*12*, *27*). Residues involved in the binding are highly conserved through the GGA family (Figure 3A). On the basis of structural superimposition with the human GGA1_GAE−WNSF motif complex, we docked the three identified GAE-binding motifs (Ent3b, Ent3c, and Ent5b) to our yGGA2_GAE domain structure (Figure 3B). As in human GAE complex structures, four highly conserved residues (A517, P519, K520, and K560) in yGGA2_GAE form a deep hydrophobic pocket for Phe0 of the bound acidic-phenylalanine motifs. It is followed by an open surface that accommodates residues at positions 1 and 2 in these motifs. A shallow pocket for position 3 is formed by a group of less conserved residues (L515, K562, and K564). Consistent with the conservation of the binding surface in yGGA2_GAE, residues at positions

1, 2, and 3 in GAE-binding motifs show higher variance compared to Phe0, although a long hydrophobic side chain residue (Phe or Met) is preferred at position 3. As in the human GGA proteins, Phe0 contributes greatly to the binding of Ent3b, Ent3c, and Ent5b motifs to the yGGA2_GAE domain (*7*, *12*) and is likely to be the major positive determinant for their interaction.

However, because Phe0 is present in all five acidic-phenylalanine motifs in Ent3 and Ent5 and because the pocket for Phe0 is invariant among the different GAE domains, determinant(s) for their binding specificity must be at other positions. To characterize the potential site determining these specificities, we conducted further mutagenesis analysis.

Positions 1 and 3 Specify the Binding of Ent3 and Ent5 Acidic-Phenylalanine Motifs to yGGA2_GAE. Further inspection of the yGGA2_GAE complex models indicated side chains of residues at positions 1 and 3 of the acidic-phenylalanine motifs formed close contacts with the GAE domain. In contrast, side chains of residues at positions 2, 4, and 5 are facing away from the GAE domain. It is suggested that residues at positions 1 and 3 might play a role in the interaction of acidic-phenylalanine motifs of Ent3 and Ent5 with yGGA2_GAE. Furthermore, we noticed that in Ent5a an Asp occupies position 3, where long hydrophobic residues predominate. To check if Asp3 affects the binding of Ent5a to yGGA2_GAE, we switched this Asp3 to the corresponding residue in Ent5b (Phe3) and tested this mutant Ent5a (DDDEFDA*F*ADG, Ent5a_D3F). Surprisingly, Ent5a_D3F gained the interaction with the yGGA2_GAE domain in an ITC experiment, with an affinity even higher than those of other active GAE-binding motifs [K_d = 0.4 ± 0.2 μM (Figure 3C)]. From the docking model, the lack of Ent5a−GAE binding is likely due to the polar-hydrophobic repulsion of the binding pocket with Asp3. Therefore, position 3 is the major negative determinant for Ent5a−yGGA2_GAE interaction.

For Ent3a, both of the residues at positions 0 and 3 are Phe residues. The determinant for Ent3a not binding to yGGA2_GAE has to be at other positions. We set out to construct several polypeptide chains by switching the sequence of Ent3b back to that of Ent3a and tested their binding to yGGA2_GAE (Figure S2 of the Supporting Information). None of them has an apparent effect on the binding of Ent3b to yGGA2_GAE, except for one substitution at position 1. Ent3b_S1 V (DDDEFVEFQSE) dramatically decreased the level of yGGA2_GAE binding [> 100-fold (Figure 3C)]. In the docking model, residue Ser1 of Ent3b points to a hydrophilic surface, formed by the main chain carbonyl group of V518, P519, K520, and M522 (Figure 3B). The OH group of Ser1 formed a direct hydrogen bond with the carbonyl group of V518 (3 Å). The steric hindrance between the larger and hydrophobic Val at position 1 could cause the repulsion of Ent3a from binding to yGGA2_GAE. In this case, position 1 is the negative determinant for Ent3a−yGGA2_GAE interaction.

DISCUSSION

The E/ANTH domain proteins Ent3 and Ent5 localize to TGN and early endosomes intimately involved in clathrin function (*7*). They have distinct roles, but both interact in vivo with yGGA2 (*11*). The interaction mechanism between yGGA2 and Ent3 and Ent5 seems to be an important link to differentiate the functions of Ent3 and Ent5. In this work, we determined that two of the three acidic-phenylalanine motifs from Ent3 are able to bind the yGGA2_GAE domain independently, while only one of two motifs from Ent5 can bind. Each potential GAE-binding motif is separated from each other with 30−100 residues; therefore, the binding for each motif might not be synergistic. The contribution of each motif to the Ent3− or Ent5−yGGA2 binding would correlate with the affinity of each motif for the GAE domain. On the basis of analysis of designed mutants in ITC experiments, we suggested a bulky hydrophobic residue at position 3 is essential for the yGGA2_GAE-binding motif. A polar residue at position 3 is the major negative determinant for Ent5a−yGGA2_GAE interaction. On the other hand, the larger and hydrophobic Val at position 1 could cause the repulsion of Ent3a from yGGA2_GAE, forming another negative determinant. Furthermore, the experimental results show consistency with on-chip simulation, indicating the side chain interaction observed in the models could represent the actual interaction.

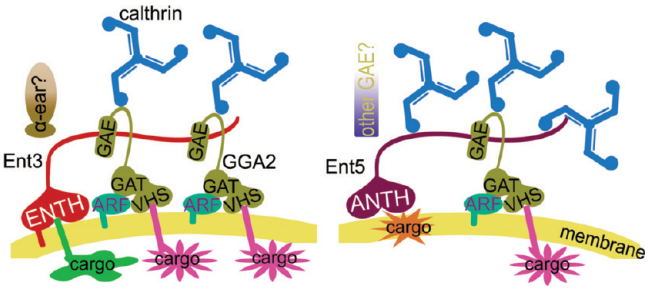

FIGURE 4: Difference between Ent3 and Ent5 in associating with clathrin-related vesicles. Ent3 and Ent5 may work differently with adaptor protein yGGA2 in clathrin-coated vesicle transportation. Without the clathrin-binding motif, Ent3 might bind to clathrin only through yGGA2 using its two functional yGGA2_GAE-binding motifs. Localization of Ent3, and even sorting pep12 by Ent3, is yGGA2-dependent. Ent5 has only one functional yGGA2_GAE-binding motif but has two clathrin-binding motifs. Therefore, clathrin binding and localization of Ent5 are not yGGA2-dependent. AP-1 also helps to determine Ent5's localization. Some other factors could contribute to this process. For example, there is a potential α-ear-binding motif in Ent3.

Although Ent3 functions as a cargo adaptor protein, it lacks a clathrin-binding motif. Its assembly on the clathrin vesicle would require the help of GGA2 and/or other adaptors. From our results, it is likely that one Ent3 will bind up to two yGGA2 molecules and bring together two clathrin triskelions, each of which binds to the hinge region of a distinct yGGA2 molecule. In contrast, Ent5 carries a lysine-rich ANTH-like phosphoinositide-binding domain (instead of an ENTH domain as in Ent3) and is unlikely to promote membrane curvature (*8*). At the same time, Ent5 has two clathrin-binding motifs that allow its direct association with clathrin (*7*, *30*). Thus, the single yGGA2_GAE-binding motif in Ent5 might not be responsible for tethering Ent5 onto the clathrin skeleton; instead, it may allow Ent5 to join the yGGA2-dependent process and take other factors to promote membrane curvature (Figure 4). Consistently, it was shown that the localization of Ent3 requires yGGA2, but Ent5 retained its localization in cells lacking Ap-1, yGGA2, or both (*11*). It is also possible that the acidic-phenylalanine motif Ent5a incapable of binding to yGGA2_GAE may bind to other GAE/ear domains and help to localize Ent5 when AP-1 and GGA proteins are knocked out. Interestingly, Ent3a also fits to the FxDxF motif that is considered to bind to the α-ear domain (*31*). It would be interesting to see if these acid-phenylalanine motifs have been fine-tuned to connect different adaptors together.

ACKNOWLEDGMENT

We appreciate the assistance in the experimental design and paper writing of Dr. Min Guo. We sincerely thank Prof. Yuhui Dong (BSRF) and Prof. Jianhua He (SSRF) for their technical assistance during data collection. We also thank Dr. Bo Ding for his help with the docking simulation.

SUPPORTING INFORMATION AVAILABLE

Summary of the constructs used in the binding assays (Table S1), graph showing that the yGGA2_GAE domain is a monomer in solution (Figure S1), and scanning mutagenesis showing position 1 is the major negative determinant in Ent3a (Figure S2). This material is available free of charge via the Internet at http://pubs.acs.org.

REFERENCES

1. Fotin, A., Cheng, Y., Sliz, P., Grigorieff, N., Harrison, S. C., Kirchhausen, T., and Walz, T. (2004) Molecular model for a complete clathrin lattice from electron cryomicroscopy. *Nature 432*, 573–579.
2. Owen, D. J., Collins, B. M., and Evans, P. R. (2004) Adaptors for clathrin coats: Structure and function. *Annu. Rev. Cell Dev. Biol. 20*, 153–191.
3. Hirst, J., Lui, W. W., Bright, N. A., Totty, N., Seaman, M. N., and Robinson, M. S. (2000) A family of proteins with γ-adaptin and VHS domains that facilitate trafficking between the trans-Golgi network and the vacuole/lysosome. *J. Cell Biol. 149*, 67–80.
4. Hirst, J., Lindsay, M. R., and Robinson, M. S. (2001) GGAs: Roles of the different domains and comparison with AP-1 and clathrin. *Mol. Biol. Cell 12*, 3573–3588.
5. Collins, B. M., Praefcke, G. J., Robinson, M. S., and Owen, D. J. (2003) Structural basis for binding of accessory proteins by the appendage domain of GGAs. *Nat. Struct. Biol. 10*, 607–613.
6. Costaguta, G., Stefan, C. J., Bensen, E. S., Emr, S. D., and Payne, G. S. (2001) Yeast Gga coat proteins function with clathrin in Golgi to endosome transport. *Mol. Biol. Cell 12*, 1885–1896.
7. Duncan, M. C., Costaguta, G., and Payne, G. S. (2003) Yeast epsin-related proteins required for Golgi-endosome traffic define a γ-adaptin ear-binding motif. *Nat. Cell Biol. 5*, 77–81.
8. Duncan, M. C., and Payne, G. S. (2003) ENTH/ANTH domains expand to the Golgi. *Trends Cell Biol. 13*, 211–215.
9. Chidambaram, S., Zimmermann, J., and von Mollard, G. F. (2008) ENTH domain proteins are cargo adaptors for multiple SNARE proteins at the TGN endosome. *J. Cell Sci. 121*, 329–338.
10. Copic, A., Starr, T. L., and Schekman, R. (2007) Ent3p and Ent5p exhibit cargo-specific functions in trafficking proteins between the trans-Golgi network and the endosomes in yeast. *Mol. Biol. Cell 18*, 1803–1815.
11. Costaguta, G., Duncan, M. C., Fernandez, G. E., Huang, G. H., and Payne, G. S. (2006) Distinct roles for TGN/endosome epsin-like adaptors Ent3p and Ent5p. *Mol. Biol. Cell 17*, 3907–3920.
12. Miller, G. J., Mattera, R., Bonifacino, J. S., and Hurley, J. H. (2003) Recognition of accessory protein motifs by the γ-adaptin ear domain of GGA3. *Nat. Struct. Biol. 10*, 599–606.
13. Lui, W. W., Collins, B. M., Hirst, J., Motley, A., Millar, C., Schu, P., Owen, D. J., and Robinson, M. S. (2003) Binding partners for the COOH-terminal appendage domains of the GGAs and γ-adaptin. *Mol. Biol. Cell 14*, 2385–2398.
14. Mattera, R., Arighi, C. N., Lodge, R., Zerial, M., and Bonifacino, J. S. (2003) Divalent interaction of the GGAs with the Rabaptin-5-Rabex-5 complex. *EMBO J. 22*, 78–88.
15. Mills, I. G., Praefcke, G. J., Vallis, Y., Peter, B. J., Olesen, L. E., Gallop, J. L., Butler, P. J., Evans, P. R., and McMahon, H. T. (2003) EpsinR: An AP1/clathrin interacting protein involved in vesicle trafficking. *J. Cell Biol. 160*, 213–222.
16. Walter, T. S., Meier, C., Assenberg, R., Au, K. F., Ren, J., Verma, A., Nettleship, J. E., Owens, R. J., Stuart, D. I., and Grimes, J. M. (2006) Lysine methylation as a routine rescue strategy for protein crystallization. *Structure 14*, 1617–1622.
17. Otwinowski, Z., and Minor, W. (1997) Processing of X-ray diffraction data collected in oscillation mode. *Methods Enzymol. 276*, 307–326.
18. Terwilliger, T. C., and Berendzen, J. (1999) Automated MAD and MIR structure solution. *Acta Crystallogr. D55*, 849–861.
19. Terwilliger, T. C. (2003) Automated main-chain model building by template matching and iterative fragment extension. *Acta Crystallogr. D59*, 38–44.
20. Vagin, A., and Teplyakov, A. (1997) Molrep: An automated program for molecular replacement. *J. Appl. Crystallogr. 30*, 1022–1025.
21. Emsley, P., and Cowtan, K. (2004) Coot: Model-building tools for molecular graphics. *Acta Crystallogr. D60*, 2126–2132.
22. Brunger, A. T., Adams, P. D., Clore, G. M., DeLano, W. L., Gros, P., Grosse-Kunstleve, R. W., Jiang, J. S., Kuszewski, J., Nilges, M., Pannu, N. S., Read, R. J., Rice, L. M., Simonson, T., and Warren, G. L. (1998) Crystallography & NMR system: A new software suite for macromolecular structure determination. *Acta Crystallogr. D54*, 905–921.
23. Murshudov, G., Vagin, A., and Dodson, E. (1997) Refinement of macromolecular structures by the maximum-likelihood method. *Acta Crystallogr. D53*, 240–255.
24. Winn, M. D., Isupov, M. N., and Murshudov, G. N. (2001) Use of TLS parameters to model anisotropic displacements in macromolecular refinement. *Acta Crystallogr. D57*, 122–133.
25. Laskowski, R. A., MacArthur, M. W., Moss, D. S., and Thornton, J. M. (1993) PROCHECK: A program to check the stereochemical quality of protein structures. *J. Appl. Crystallogr. 26*, 283–291.
26. Van Der Spoel, D., Lindahl, E., Hess, B., Groenhof, G., Mark, A. E., and Berendsen, H. J. (2005) GROMACS: Fast, flexible, and free. *J. Comput. Chem. 26*, 1701–1718.
27. Inoue, M., Shiba, T., Ihara, K., Yamada, Y., Hirano, S., Kamikubo, H., Kataoka, M., Kawasaki, M., Kato, R., Nakayama, K., and Wakatsuki, S. (2007) Molecular basis for autoregulatory interaction between GAE domain and hinge region of GGA1. *Traffic 8*, 904–913.
28. Dell'Angelica, E. C., Puertollano, R., Mullins, C., Aguilar, R. C., Vargas, J. D., Hartnell, L. M., and Bonifacino, J. S. (2000) GGAs: A family of ADP ribosylation factor-binding proteins related to adaptors and associated with the Golgi complex. *J. Cell Biol. 149*, 81–94.
29. Kent, H. M., McMahon, H. T., Evans, P. R., Benmerah, A., and Owen, D. J. (2002) γ-Adaptin appendage domain: Structure and binding site for Eps15 and γ-synergin. *Structure 10*, 1139–1148.
30. Dell'Angelica, E. C. (2001) Clathrin-binding proteins: Got a motif? Join the network!. *Trends Cell Biol. 11*, 315–318.
31. Legendre-Guillemin, V., Wasiak, S., Hussain, N. K., Angers, A., and McPherson, P. S. (2004) ENTH/ANTH proteins and clathrin-mediated membrane budding. *J. Cell Sci. 117*, 9–18.